

# A preconditioning approach for improved estimation of sparse polynomial chaos expansions

Negin Alemazkoor, Hadi Meidani

*Department of Civil and Environmental Engineering, University of Illinois at Urbana-Champaign, Urbana, Illinois, USA.*

---

## Abstract

Compressive sampling has been widely used for sparse polynomial chaos (PC) approximation of stochastic functions. The recovery accuracy of compressive sampling depends on the coherence properties of measurement matrix. In this paper, we consider preconditioning the measurement matrix. Premultiplying a linear equation system by a non-singular matrix results in an equivalent equation system, but it can impact the coherence properties of preconditioned measurement matrix and lead to a different recovery accuracy. In this work, we propose a preconditioning scheme that significantly improves the coherence properties of measurement matrix, and using theoretical motivations and numerical examples highlight the promise of the proposed approach in improving the accuracy of estimated polynomial chaos expansions.

---

## 1. Introduction

Reliable analysis of natural and engineered systems necessitates the understanding of how the system response or quantity of interest (QoI) depends on uncertain inputs. Uncertainty quantification (UQ) tackles these issues with efficient propagation of input uncertainties onto the QoI. This is typically done by building approximate surrogates that replace computationally expensive simulations. Surrogates approximate QoI as an analytical function of random inputs and facilitate quantifying parametric uncertainty. As a widely used spectral surrogate, polynomial chaos expansion (PCE) uses orthogonal polynomials for the approximation of QoI. In order to construct PCEs, i.e. determine the expansion coefficients corresponding to different polynomial bases, the most widely used approach is stochastic collocation. This approach is advantageous particularly because it is nonintrusive and easy to implement by reusing legacy codes. Examples of stochastic collocation methods include spectral projection [1, 2], sparse grid interpolation [3, 4], and least square [5, 6]. The outstanding challenge is that the number of sample points that these methods require for accurate prediction increases drastically as the number of uncertain inputs, or the dimension of the PCE, increases.

Recently, motivated by the fact that approximated PCE for high dimensional problems is sparse, compressive sampling has been effectively used to approximate PCE coefficients with a small number of simulations and alleviate the dimensionality-related challenge [7, 8, 9, 10, 11, 12]. The accuracy of sparse polynomial approximation heavily relies on incoherence properties of measurement matrix that consists of evaluated polynomial bases at sample points. Most commonly, in standard sampling, samples are generated randomly from the probability distribution of random inputs. Recently, other sampling strategies have been proposed in order to improve the accuracy of sparse PCEs. In [13], in construction of sparse Legendre-based PCE, it was proposed to draw samples from Chebyshev probability distribution. The theoretical and numerical results in [9] showed that Chebyshev sampling deteriorates the recovery accuracy in high dimensional problems. Drawing samples randomly from the tensor grid of Gaussian quadrature points was recommended in [8, 14]. Although the results showed significant accuracy improvement in low-dimensional problems, the results underperformed or were close to standard sampling in high-dimensional problems. A sampling strategy that outperforms standard sampling in both low-dimensional high-order and high-dimensional low-order problems was proposed in [15], and was called the coherence-optimal sampling. In coherence-optimal sampling, samples are drawn from a measure that minimizes the (local) coherence of orthogonal polynomial system. In [10], a near-optimal sampling strategy was proposed, which further improved coherence-optimal sampling by selecting from the pool of coherence-optimal samples, the ones that lead to a measurement with better cross-correlation properties.

In this work, instead of relying on experimenting with sampling strategies to improve the incoherence properties of measurement matrix, we take a new approach and use a preconditioning scheme to enhance these

properties. Using theoretical reasoning and numerical examples, it will be demonstrated that preconditioning can significantly improve the accuracy of PCE using compressive sampling. This paper is organized as follows: Section 2 provides a brief overview on application of compressive sampling in PCE approximation; Section 3 introduced the preconditioning scheme along with the theoretical motivation and Section 4 includes numerical illustration and detailed discussion about the results of the preconditioning approach.

## 2. Setup and background

### 2.1. Polynomial chaos expansion

Consider the vector of independent random variables  $\Xi = (\Xi_1, \dots, \Xi_d)$  to be  $d$  system random inputs and  $u(\Xi)$  to be the uncertain QoI with finite variance. Then,  $u(\Xi)$  can be written as an expansion of orthogonal polynomials, i.e.

$$u(\Xi) = \sum_{\alpha \in \mathbb{N}_0^d} c_{\alpha} \psi_{\alpha}(\Xi). \quad (1)$$

Let  $I_{\Xi} \subseteq \mathbb{R}^d$  be a tensor-product domain that is the support of  $\Xi$ , i.e.  $\Xi_i \in I_{\Xi_i}$  and  $I_{\Xi} = \times_{i=1}^d I_{\Xi_i}$ . Also, let  $\rho_i : I_{\Xi_i} \rightarrow \mathbb{R}^+$  be the probability measure for variable  $\Xi_i$  and let  $\rho(\Xi) = \prod_{i=1}^d \rho_i(\Xi_i)$ . Given this setting, the set of univariate orthonormal polynomials,  $\{\psi_{\alpha,i}\}_{\alpha \in \mathbb{N}_0}$ , satisfies

$$\int_{I_{\Xi_i}} \psi_{n,i}(\xi_i) \psi_{m,i}(\xi_i) \rho_i(\xi_i) d\xi_i = \delta_{mn}, \quad m, n \in \mathbb{N}_0. \quad (2)$$

Consequently, the  $d$ -dimensional orthonormal polynomials  $\{\psi_{\alpha}\}_{\alpha \in \mathbb{N}_0^d}$  in  $\Xi$  are formed by the product of the univariate orthonormal polynomials,

$$\psi_{\alpha}(\Xi) = \prod_{i=1}^d \psi_{\alpha_i,i}(\Xi_i), \quad (3)$$

where  $\alpha_i$  represents the  $i$ th coordinate of  $\alpha$ . For practicality, we need to truncate the expansion in (1) by limiting the total order of polynomial to be  $k$  and only including bases with  $\|\alpha\|_1 \leq k$  in the expansion. The cardinality of basis set, denoted by  $K$ , will then be

$$K := \frac{(k+d)!}{k! d!}. \quad (4)$$

The resulting truncated PCE,  $u_k(\Xi)$ , offers a practical approximation of  $u(\Xi)$  (inducing a truncation error),

$$u(\Xi) \approx u_k(\Xi) := \sum_{\|\alpha\|_1 \leq k} c_{\alpha} \psi_{\alpha}(\Xi). \quad (5)$$

The exact PCE coefficients in Eq. 6 can be exactly calculated by projecting  $u(\Xi)$  onto the basis functions  $\psi_{\alpha}$ :

$$c_{\alpha} = \mathbb{E}_{\rho} [u(\Xi) \psi_{\alpha}(\Xi)] = \int_{I_{\Xi}} u(\xi) \psi_{\alpha}(\xi) \rho(\xi) d\xi. \quad (6)$$

In the typical absence of analytical solution for this multidimensional integral, the PCE coefficients can be numerically calculated using non-intrusive approaches such as Monte Carlo sampling and sparse grid quadrature [16]. However, it is known that Monte Carlo sampling converges slowly and sparse grid quadrature can be impractical in high-dimensional problems [16, 17]. In practice, for high-dimensional problems, least squares regression is widely used for the calculation of PCE coefficients. This approach requires the number of samples to be larger than the number of unknown coefficients, in order to make the system of equations overdetermined. The generally accepted oversampling rate is about 1.5 to 3 times the number of coefficients [18, 5]. Recently, a quasi-optimal sampling approach was introduced in [5] that allows accurate coefficient recovery with  $\mathcal{O}(1)$  samples. However, affording that many samples may still be computationally impossible. In [7] it was shown that when the QoI is sparse with respect to the PCE bases, compressive sampling can be used to calculate the coefficients using significantly smaller number of samples than coefficients. This section follows with a brief introduction of compressive sampling application in PCE approximation.

## 2.2. Sparse PCE estimation via compressive sampling

Compressive sampling first emerged in field of signal possessing and has since found applications in various domains, such as radar systems [19], speech recognition [20] and MR imaging [21]. Compressive sampling solves an under-determined system of equations by exploring its sparsest solution. Here, we present the compressive sampling in the context of stochastic collocation. Specifically, consider  $M$  realizations  $\{\boldsymbol{\xi}^{(i)}\}_{i=1}^M$  of system input, with corresponding model outputs  $\mathbf{u} = (u(\boldsymbol{\xi}^{(1)}), \dots, u(\boldsymbol{\xi}^{(M)}))^T$ . We seek a solution that satisfies

$$\boldsymbol{\Psi}\mathbf{c} = \mathbf{u}, \quad (7)$$

where  $\boldsymbol{\Psi}$  is the Vendermonde-like matrix, often referred to measurement or design matrix, and is constructed according to

$$\boldsymbol{\Psi} = [\psi_{ij}], \quad \psi_{ij} = \psi_{\boldsymbol{\alpha}^j}(\boldsymbol{\xi}^{(i)}), \quad 1 \leq i \leq M, \quad 1 \leq j \leq K. \quad (8)$$

The problem 7 is under-determined and ill-posed when  $M < K$ . Therefore, obtaining a unique solution requires adding some regulations to the problem. In compressive sampling, the ideal goal is to determine the sparsest solution, which can be achieved by minimizing the  $\ell_0$ -norm of solution according to

$$\min_{\mathbf{c}} \|\mathbf{c}\|_0 \quad \text{subject to} \quad \boldsymbol{\Psi}\mathbf{c} = \mathbf{u}. \quad (9)$$

However, since  $\ell_0$ -norm is non-convex and discontinuous, the above problem is NP-hard. Therefore,  $\ell_0$  minimization is usually replaced with its convex relaxation, where the  $\ell_1$ -norm of solution  $\mathbf{c}$  is minimized instead, i.e.

$$\min_{\mathbf{c}} \|\mathbf{c}\|_1 \quad \text{subject to} \quad \boldsymbol{\Psi}\mathbf{c} = \mathbf{u}. \quad (10)$$

Under certain conditions,  $\ell_1$  minimization gives the same solution as  $\ell_0$  minimization [22]. The  $\ell_1$  minimization problem is commonly known as *Basis Pursuit*. Other types of regulations such as *Basis Pursuit Denoising*, *Least Absolute Shrinkage and Selection Operator*,  $\ell_{1-2}$  minimization and  $\ell_{0.5}$  regulation can also be used [23, 24, 25, 26, 27]

## 2.3. $\ell_1$ minimization recoverability

The ability of  $\ell_1$  minimization in accurate solution recovery depends on the actual sparsity of solution  $\mathbf{c}$  and properties of measurement matrix  $\boldsymbol{\Psi}$ . Here, we discuss one of the main properties of  $\boldsymbol{\Psi}$ , shown to be significantly relevant to recovery accuracy.

**Definition 1.** (restricted isometry constant [28]) *The  $s$ -restricted isometry constant for a matrix  $\boldsymbol{\Psi} \in \mathbb{R}^{M \times K}$  is defined to be the smallest  $\delta_s \in (0, 1)$  such that*

$$(1 - \delta_s) \|\mathbf{c}\|_2^2 \leq \|\boldsymbol{\Psi}\mathbf{c}\|_2^2 \leq (1 + \delta_s) \|\mathbf{c}\|_2^2, \quad (11)$$

for all  $\mathbf{c} \in \mathbb{R}^K$  that are at most  $s$ -sparse.

Depending on the property of this isometry constant, one can expect the  $\ell_1$  minimization (10) to produce a very accurate and even exact solution, as stated in the following theorem.

**Theorem 1** ([28]). *Let  $\boldsymbol{\Psi} \in \mathbb{R}^{M \times K}$  with isometry constant  $\delta_{2s}$  such that  $\delta_{2s} < \sqrt{2} - 1$ . For a given  $\bar{\mathbf{c}}$ , and measurement  $\mathbf{y} = \boldsymbol{\Psi}\bar{\mathbf{c}}$ , let  $\mathbf{c}$  be the solution of*

$$\min \|\mathbf{c}\|_1 \quad \text{subject to} \quad \boldsymbol{\Psi}\mathbf{c} = \mathbf{y}. \quad (12)$$

*Then the reconstruction error satisfies*

$$\|\mathbf{c} - \bar{\mathbf{c}}\| \leq C_1 \frac{\|\bar{\mathbf{c}} - \mathbf{c}^*\|}{\sqrt{s}} \quad (13)$$

where  $C_1$  only depends on  $\delta_{2s}$  and  $\mathbf{c}^*$  is the vector  $\bar{\mathbf{c}}$  with all but the  $s$ -largest entries set to be zero. If  $\bar{\mathbf{c}}$  is  $s$ -sparse, then the recovery is exact.

Since calculating the isometry constant is an NP-complete problem, one can use the following theorem which provides a probabilistic upperbound on the isometry constant for bounded orthonormal systems. An

orthonormal system  $\{\psi_n\}_{1 \leq n \leq K}$  with respect to density  $\rho(\xi)$  is a bounded orthonormal system if it satisfies

$$\sup_{1 \leq n \leq K} \|\psi_n\|_\infty = \sup_{1 \leq n \leq K} \sup_{\xi \in \text{supp}(\rho)} |\psi_n(\xi)| \leq L. \quad (14)$$

**Theorem 2** ([29]). *Let  $\{\psi_n\}_{1 \leq n \leq K}$  be a bounded orthonormal system. Also let  $\Psi \in \mathbb{R}^{M \times K}$  be a measurement matrix with entries  $\{\psi_{ij} = \psi_j(\xi^{(i)})\}_{1 \leq i \leq M, 1 \leq j \leq K}$ , where  $\xi^{(1)}, \dots, \xi^{(M)}$  are random samples drawn from measure  $\rho$ . Assuming that*

$$M \geq C \delta^{-2} L^2 s \log^3(s) \log(K), \quad (15)$$

*then with probability at least  $1 - K^{\beta \log^3(s)}$ , the isometry constant  $\delta_s$  of  $\frac{1}{\sqrt{M}} \Psi$  satisfies  $\delta_s \leq \delta$ .  $C, \beta > 0$  are universal constants.*

Hereinafter, let us refer to bound  $L$  as local-coherence. In highly over-determined cases, for large values of  $M$ ,  $\Psi$  will be asymptotically a matrix with near column-orthogonality. Local-coherence can be seen as a measure of how concentrated the rows of asymptotic  $\Psi$  are. Consider the under-determined  $\Psi$  as a row-subsample of an asymptotical  $\Psi$  (i.e. one with a very large  $M$ ). When the local-coherence, i.e. row-concentration, is large, it is expected that some of the rows in the asymptotical  $\Psi$  have a more significant role in maintaining the column-orthogonality. Therefore, if in row-subsampling the asymptotical  $\Psi$ , these “significant” rows are not selected, the resulting under-determined  $\Psi$  will have poor column-orthogonality conditions.

#### 2.4. Coherence-optimal and near-optimal sampling

Coherence-optimal sampling was introduced in [15] and was motivated by Theorem 2. In this approach, instead of directly sampling from the probability measure,  $\rho(\xi)$ , samples are drawn from a different “optimal” probability measure,  $\rho_o(\xi)$ , which was shown to result in the lowest local-coherence.  $\rho_o(\xi)$  is constructed according to

$$\rho_o(\xi) = C^2 \rho(\xi) B^2(\xi), \quad (16)$$

where  $C$  is a normalizing constant and

$$B(\xi) := \max_{\|\alpha\|_1 \leq k} |\psi_\alpha(\xi)|. \quad (17)$$

Corresponding to this new probability measure, the weight function used to maintain the orthogonality of polynomial bases should be

$$w(\xi) = \frac{1}{B(\xi)}. \quad (18)$$

Accordingly, the following weighted  $\ell_1$ -minimization is used for sparse recovery

$$\min_{\mathbf{c}} \|\mathbf{c}\|_1 \quad \text{subject to} \quad \mathbf{W} \Psi \mathbf{c} = \mathbf{W} \mathbf{u}, \quad (19)$$

where  $\mathbf{W}$  is the  $M \times M$  diagonal weight matrix, with  $\mathbf{W}(i, i) = w(\xi^{(i)})$  for  $i = 1, \dots, M$ .

It has been shown that coherence-optimal sampling can significantly improve the accuracy of sparse recovery for PCE [15]. In [10], a near-optimal sampling approach was proposed, which aimed to simultaneously improve the local-coherence and the cross-correlation properties of the resulting measurement matrix. In this approach, first a large pool of sample candidates are drawn from the coherence-optimal sampling distribution, out of which the final sample set of size  $M$  is selected such that the cross-correlation properties of the resulting measurement matrix are improved. Numerical examples have shown that near-optimal sampling can significantly improve the accuracy of sparse PCE recovery for problems with various combinations of dimensionality and response order.

In this work, we introduce an alternative preconditioning approach for improving the properties of measurement matrix, by proposing preconditioning. This approach can also address the case where samples have already been drawn using expensive simulations or costly experiments and sampling strategies have become inapplicable. The term *preconditioning* has already been used in the sparse PCE approximation literature, referring the weight matrix that preserves asymptotic orthogonality of basis functions for non-standard sampling distributions [30, 15]. In under-determined cases, where a limited set of samples are available, enforcing asymptotic orthogonality does not guarantee improvement in the coherence properties

of measurement matrices. To the best of our knowledge, this work is the first attempt at preconditioning the underdetermined measurement matrix towards optimal coherence properties.

### 3. A preconditioning scheme

In Sections 2.2, we discussed the relevant properties of the measurement matrix  $\Psi$ , that can impact the recovery accuracy. One can enhance the recovery accuracy by improving the incoherence properties of  $\Psi$  using advanced sampling strategies [15, 14, 10]. However, the question is how to enhance the properties of  $\Psi$  if this matrix has already been constructed, i.e., the samples are already drawn. Preconditioning is the answer. To this end, we multiply the measurement matrix with a preconditioner matrix,  $\mathbf{P} \in \mathbb{R}^{M \times M}$ , such that the matrix  $\mathbf{P}\Psi$  is less coherent than the original measurement matrix. Consequently, we solve the following  $\ell_1$ -minimization

$$\min_{\mathbf{c}} \|\mathbf{c}\|_1 \quad \text{subject to} \quad \mathbf{P}\Psi\mathbf{c} = \mathbf{P}\mathbf{u}. \quad (20)$$

The weight matrix in (19) can be thought of as a preconditioner matrix, which improves the properties of the measurement matrix. However, by definition it is a diagonal matrix, with its diagonal terms  $w(i, i)$  being a function of the  $i$ th sample location. We do not impose the diagonal constraint on  $\mathbf{P}$  and do not constrain it to be the function of sample locations.

Let define  $\mathbf{D} \triangleq \mathbf{P}\Psi \in \mathbb{R}^{M \times K}$  and call it *equivalent measurement matrix*. Properties of  $\mathbf{D}$  significantly impact the recovery accuracy. One of the main properties of  $\mathbf{D}$  that directly impacts the recovery accuracy is its spark. The spark of a matrix is the smallest number of its columns that are linearly dependent.  $\ell_1$  minimization is guaranteed to recover an  $s$ -sparse signal vector if  $\text{spark}(\mathbf{D}) > 2s$ . Designing preconditioning matrix such that the spark of the equivalent measurement matrix is maximized would allow the exact recovery of a larger set of signals. However, computing the spark of a matrix is an NP-hard problem. Alternatively, one can analyze recovery guarantees using other properties which are easier to compute. One such property is the mutual coherence, which for a given matrix is defined as the maximum absolute normalized inner product, i.e. cross-correlation, between its columns [7, 31]. Let  $D_1, D_2, \dots, D_K \in \mathbb{R}^M$  be the columns of matrix  $\mathbf{D}$ . The mutual coherence of matrix  $\mathbf{D}$ , denoted by  $\mu(\mathbf{D})$ , is then given by

$$\mu(\mathbf{D}) := \max_{1 \leq i, j \leq K, i \neq j} \frac{|D_j^T D_i|}{\|D_j\|_2 \|D_i\|_2}. \quad (21)$$

Mutual coherence gives a lower bound for spark as follows [32]

$$\text{spark}(\mathbf{D}) \geq 1 + \frac{1}{\mu(\mathbf{D})}. \quad (22)$$

It may be concluded that preconditioning matrix  $\mathbf{P}$  should be designed in a way that mutual coherence of  $\mathbf{D}$  is minimized. However, it has been observed that minimizing mutual coherence does not necessarily improve the recovery accuracy of compressive sampling [33, 34]. This is because Equation (22) only provides a lower bound on the spark. Therefore, minimizing mutual coherence is equivalent to optimizing for the worst-case scenario and fails to reflect upon other possibilities for improving compressive sampling performance [34].

Theorem 2 suggests that optimizing the preconditioning matrix so that isometry constant of equivalent measurement matrix is minimized will be effective. However, as previously mentioned, calculating isometry constant for a given matrix is an NP-complete problem. However, if one considers all the column-submatrices of the equivalent measurement matrix that has  $s^* \leq s$  columns, it is known that the eigenvalues of these column-submatrices is bounded by the isometry constant. Therefore, one may suggest to minimize the condition number of all column-submatrices with  $s$  or fewer columns. However, calculating such combinatorial measure is not a trivial task either and can be computationally impossible [34].

As a result, establishing a single matrix property that is directly associated with the accuracy of compressive sampling method and is easily computable still remains an open challenge [33, 34]. To sidestep this challenge, efforts have focused on identifying properties or measures that are relatively better than the mutual coherence. For example, the average coherence of the equivalent measurement matrix can be minimized [34]. Alternatively, one can minimize the distance between the Gram matrix  $\mathbf{G} = \mathbf{D}^T \mathbf{D}$  and the identity matrix or an equiangular tight frame (ETF) Gram matrix [33, 35, 36, 37]. ETF matrices are matrices consisting of unit vectors whose maximum cross-correlation achieves the smallest possible value, and as such are ideal measurement matrices for sparse recovery. In this work, we start off by minimizing the

distance of the preconditioned Gram matrix with respect to the identity matrix, which was shown to lead to more accurate recovery [33]. In particular, we solve the following problem

$$\min_{\mathbf{P} \in \mathbb{R}^{M \times M}} \|\mathbf{I}_K - \mathbf{\Psi}^T \mathbf{P}^T \mathbf{P} \mathbf{\Psi}\|_F^2. \quad (23)$$

where  $\mathbf{I}_K$  denotes the  $K \times K$  identity matrix, and  $\|\cdot\|_F$  is the Frobenius norm. A similar problem was formulated in [33], where the optimal projection (or sensing) matrix was identified to improve the accuracy of sparse signal recovery. It has been shown that a set of solution matrices can be considered for 23. Specifically, if we consider

$$\mathcal{P}_{\text{opt}} = \arg \min_{\mathbf{P} \in \mathbb{R}^{M \times M}} \|\mathbf{I}_K - \mathbf{\Psi}^T \mathbf{P}^T \mathbf{P} \mathbf{\Psi}\|_F^2, \quad (24)$$

then, we have [33]

$$\mathcal{P}_{\text{opt}} = \{\mathbf{P} : \mathbf{P} = \mathbf{P}_{\text{opt}}(\mathbf{V}_{11}, \mathbf{V}_{\Psi}) := \mathbf{U} \mathbf{I}_M \mathbf{V}_{11}^T \mathbf{\Lambda}_{\Psi}^{-1} \mathbf{U}_{\Psi}^T\}, \quad (25)$$

where  $\mathbf{\Psi} = \mathbf{U}_{\Psi} [\mathbf{\Lambda}_{\Psi} \ 0] \mathbf{V}_{\Psi}^T$  is a Singular Value Decomposition (SVD) of  $\mathbf{\Psi}$ ,  $\mathbf{\Lambda}_{\Psi} = \text{diag}(\lambda_1, \dots, \lambda_M)$ , and  $\mathbf{V}_{11} \in \mathbb{R}^{M \times M}$  and  $\mathbf{U} \in \mathbb{R}^{M \times M}$  are arbitrary orthonormal matrices. It should be noted that Equation 25 gives a class of solutions for 23. Among the preconditioning matrices belonging to this solution class, depending on the choice of the arbitrary orthonormal matrix  $\mathbf{V}_{11}$ , the resulting equivalent measurement matrix will still have different coherence properties. We can then pursue to identify the best  $\mathbf{V}_{11}$  that leads to the smallest distance between the resulting Gram matrix and a space of ETF Gram matrices according to

$$\mathbf{V}_{11}^{\text{opt}}(\mathbf{V}_{\Psi}) = \underset{\mathbf{V}_{11}, \mathbf{G}_{\text{ETF}} \in \mathcal{G}_{\epsilon}}{\text{argmin}} \|\mathbf{G}_{\text{ETF}} - \mathbf{\Psi}^T \mathbf{P}_{\text{opt}}(\mathbf{V}_{11}, \mathbf{V}_{\Psi})^T \mathbf{P}_{\text{opt}}(\mathbf{V}_{11}, \mathbf{V}_{\Psi}) \mathbf{\Psi}\|_F, \quad (26)$$

where

$$\mathcal{G}_{\epsilon} := \{\mathbf{G} \in \mathbb{R}^{M \times M} : \mathbf{G} = \mathbf{G}^T, \mathbf{G}(i, i) = 1, \max_{i \neq j} |\mathbf{G}(i, j)| \leq \epsilon, \forall i\}, \quad (27)$$

is the space of ETF Gram matrices with constant  $\epsilon$ . This constant should be selected in such a way that  $\mathcal{G}_{\epsilon}$  includes  $M \times K$  ETF Gram matrices with ideal properties. We set  $\epsilon = \mu_{\min} = \sqrt{(K - M)/(M(K - 1))}$ , which is the lower bound for mutual coherence for a matrix in  $\mathbb{R}^{M \times K}$ . In our numerical experiment, negligible impact on the performance was observed when  $\epsilon$  was set to be slightly larger. It should be noted that since  $\mathbf{V}_{\Psi}$  belongs to an SVD of  $\mathbf{\Psi}$ , different choices of  $\mathbf{V}_{\Psi}$  can result in different optimal solutions  $\mathbf{V}_{11}^{\text{opt}}$ ; hence the notation  $\mathbf{V}_{11}^{\text{opt}}(\mathbf{V}_{\Psi})$ .

In order to minimize the distance with respect to the space of ETF Gram matrices, past efforts in the context of optimal sensing matrix have used alternating approaches [38, 35]. Building upon these works, an analytical approach was proposed in [33] and is adopted in this work to solve 26. Specifically, at the  $k$ th iteration of this approach we update, until no further improvement can be achieved, the new optimum  $\mathbf{V}_{11}^{\text{opt}(k)}$  according to

$$\mathbf{V}_{11}^{\text{opt}(k)} = \underset{\mathbf{V}_{11}}{\text{argmin}} \|\mathbf{G}_t^{(k-1)} - \mathbf{G}(\mathbf{V}_{11})\|_F, \quad (28)$$

where

$$\mathbf{G}(\mathbf{V}_{11}) = \mathbf{V}_{\Psi} \begin{bmatrix} \mathbf{V}_{11} & 0 \\ 0 & 0 \end{bmatrix} \begin{bmatrix} \mathbf{I}_M & 0 \\ 0 & 0 \end{bmatrix} \begin{bmatrix} \mathbf{V}_{11} & 0 \\ 0 & 0 \end{bmatrix} \mathbf{V}_{\Psi}^T, \quad (29)$$

and  $\mathbf{G}_t^{(k-1)}$  is obtained by shrinking  $\tilde{\mathbf{G}}^{(k-1)}$ , which is the column-normalized version of the Gram matrix  $\mathbf{G}(\mathbf{V}_{11}^{\text{opt}(k-1)})$ , according to

$$\mathbf{G}_t^{(k-1)}(i, j) = \begin{cases} \tilde{\mathbf{G}}^{(k-1)}(i, j), & \tilde{\mathbf{G}}(i, j) \leq \mu_{\min}, \\ 1, & i = j, \\ \text{sign}(\tilde{\mathbf{G}}^{(k-1)}(i, j)) \mu_{\min}, & \text{otherwise.} \end{cases} \quad (30)$$

Using Eq. 29 one can rewrite  $\|\mathbf{G}_t^{(k-1)} - \mathbf{G}(\mathbf{V}_{11})\|_F$  as

$$\left\| \mathbf{Q} - \begin{bmatrix} \mathbf{V}_{11} & 0 \\ 0 & 0 \end{bmatrix} \begin{bmatrix} \mathbf{I}_M & 0 \\ 0 & 0 \end{bmatrix} \begin{bmatrix} \mathbf{V}_{11}^T & 0 \\ 0 & 0 \end{bmatrix} \right\|_F, \quad (31)$$

where  $\mathbf{Q} = \mathbf{V}_\Psi^T \mathbf{G}_i^{(k-1)} \mathbf{V}_\Psi = \begin{bmatrix} \mathbf{Q}_{11} & \mathbf{Q}_{12} \\ \mathbf{Q}_{21} & \mathbf{Q}_{22} \end{bmatrix}$  with  $\mathbf{Q}_{11} \in \mathbb{R}^{M \times M}$ . Let  $\mathbf{Q}_{11} = \mathbf{V}_e \mathbf{\Lambda} \mathbf{V}_e^T$ , where  $\mathbf{V}_e$  consists of the eigenvector of  $\mathbf{Q}_{11}$  such that  $\mathbf{V}_e \mathbf{V}_e^T = \mathbf{I}_M$  and  $\mathbf{\Lambda} = \text{diag}(\sigma_1, \dots, \sigma_i, \dots, \sigma_M)$  with  $\sigma_i \geq \sigma_{i+1}$ . It can be then shown that [33]

$$\mathbf{V}_{11}^{\text{opt}(k)} = \mathbf{V}_e. \quad (32)$$

This approach is computationally appealing since the updates in each iteration are carried out analytically, and it avoids the computational burden imposed by gradient-based updates. We should reiterate that the resulting optimum  $\mathbf{V}_{11}^{\text{opt}}(\mathbf{V}_\Psi)$  is obtained given a specific choice of SVD for  $\mathbf{\Psi}$ , and the resulting preconditioning matrix may not be globally optimal. Having said this, the proposed preconditioning is nonetheless expected to significantly improve the incoherence properties of the equivalent measurement matrix, as will be demonstrated by the numerical examples in the next section.

## 4. Numerical illustration

To demonstrate the improvement in recovery accuracy using the preconditioning scheme, we generate Hermite and Legendre phase transition diagrams for several combinations of polynomial dimension,  $d$ , and polynomial order,  $k$ . As additional numerical examples, we also consider three target functions in this section: (i) a low-dimensional high-order polynomial function, (ii) a high-dimensional low-order polynomial function, and (iii) a six-dimensional generalized Rosenbrock function, to allow a comprehensive comparison of recovery accuracy with and without preconditioning. In all examples, optimization problems (10) and (19), corresponding to a noise-less measurement setting were formed and solved using the SPGL1 package [39].

### 4.1. Phase transition diagrams

Consider the target function to be in fact a polynomial expansion, i.e.  $f(\Xi) = \sum_{j=1}^K \mathbf{c}_{\alpha^j} \Psi_{\alpha^j}(\Xi)$ , where the known coefficient vector  $\mathbf{c}$  is exactly  $s$ -sparse. Our objective is to evaluate recoverability of  $\mathbf{c}$  using only  $M$  samples. To perform a comprehensive recoverability evaluation, we consider several scenarios with varying sparsity and sample size. Specifically, let us consider a unit square  $[0, 1]^2$ , where the x-axis shows undersampling rates,  $M/K$ , and the y-axis shows sparsity rates,  $s/M$ . This unit square, which constitutes the domain for phase transition diagrams, typically partitions into three regions: (1) a region where the probability of accurate recovery is near one; (2) a region where the probability of accurate recovery is near zero; (3) a narrow transition region [40, 41]. Furthermore, we consider scenarios where order and dimension of polynomial expansion are varied. For each choice of dimension and order, we divide the unit square to a  $50 \times 50$  grid. At each point in the grid, i.e. for each combination of  $d, k, s$  and  $M$ , we study the success rate of the  $\ell_1$ -minimization on 100 ‘‘trial’’ target expansions. Each trial target expansion is created by randomly selecting  $s$  coefficients and assigning them to values drawn from a standard normal distribution, while setting the remaining coefficients equal to zero. For each trial target expansion, the recovery is determined to be successful if  $\|\mathbf{c} - \bar{\mathbf{c}}\|_\infty < 10^{-3}$ , where  $\mathbf{c}$  is the coefficient of the target expansion and  $\bar{\mathbf{c}}$  is the solution of the  $\ell_1$ -minimization. The recovery probability is then defined as the ratio of successful recoveries among all recoveries for the 100 trial target expansions. Finally, the transition diagrams are created by connecting the points at which the successful recovery probability is estimated to be 50%. In this work, we compare phase transition diagrams for standard and coherence-optimal sampling with and without preconditioning.

Figure 1 includes the phase transition diagrams for 6 combinations of dimension and order for Legendre-based target expansions and shows that preconditioning significantly improves the recovery accuracy. In cases where  $d \ll k$  or  $k \approx d$  preconditioned coherence-optimal sampling outperforms preconditioned standard sampling. This is because coherence-optimal sampling is expected to outperform standard sampling more significantly in these cases, and as the dimensionality increases and the polynomial order decreases the coherence-optimal sampling distribution becomes similar to uniform distribution. This can be explained by referring to the coherence-optimal distribution given by  $\rho_o(\xi) = C^2 \rho(\xi) B^2(\xi)$ , where  $C$  is a normalizing constant and  $B(\xi)$  is the largest absolute value of all the polynomial bases as a function of  $\xi$ . For Legendre-based expansions,  $\rho_o(\xi) \propto B^2(\xi)$ . For  $d \ll k$  or  $d \approx k$ , this distribution is expected to peak when  $\xi$  values in all dimensions are close to the boundary. To explain this, we note that one-dimensional degree- $\alpha_i$  Legendre polynomials reach their maximum absolute values at their support boundaries, and that  $B(\xi_i) \leq (2\alpha_i + 1)^{\frac{1}{2}}$

[9]. Therefore, for  $d$ -dimensional Legendre polynomials with the multi-index  $\alpha$ , we have

$$B(\xi) \leq \prod_{i=1}^d (2\alpha_i + 1)^{\frac{1}{2}}. \quad (33)$$

When  $d \ll k$ , the expansion will include full-dimensional bases (where all the dimensions are present) and therefore  $B(\xi)$  is peaked when  $\xi$  values in all dimensions are close to the boundary. However, when  $d \gg k$ , the expansion will not include full-dimensional bases; it will have at most  $k$ -dimensional bases, and the full-dimensional bound of Eq. 33 will never be triggered. As a result,  $B(\xi)$  is peaked at samples of  $\xi$  that have  $k$  entries close to the boundary, and the remaining  $K - k$  entries can be randomly located anywhere in the parameter space. Consequently, for large values of  $d$  and small values of  $k$ ,  $\rho_o(\xi)$  becomes similar to uniform distribution and coherence-optimal sampling produces results similar to those obtained by standard sampling.

Figure 2 includes the phase transition diagrams for Hermite polynomial functions considering the same combinations of dimensionality and order. Again, it can be seen that advantage of coherence-optimal sampling over standard sampling disappears when target solutions become higher-dimensional and lower-order. Also, we observe that in all cases preconditioning significantly improves the recovery accuracy.



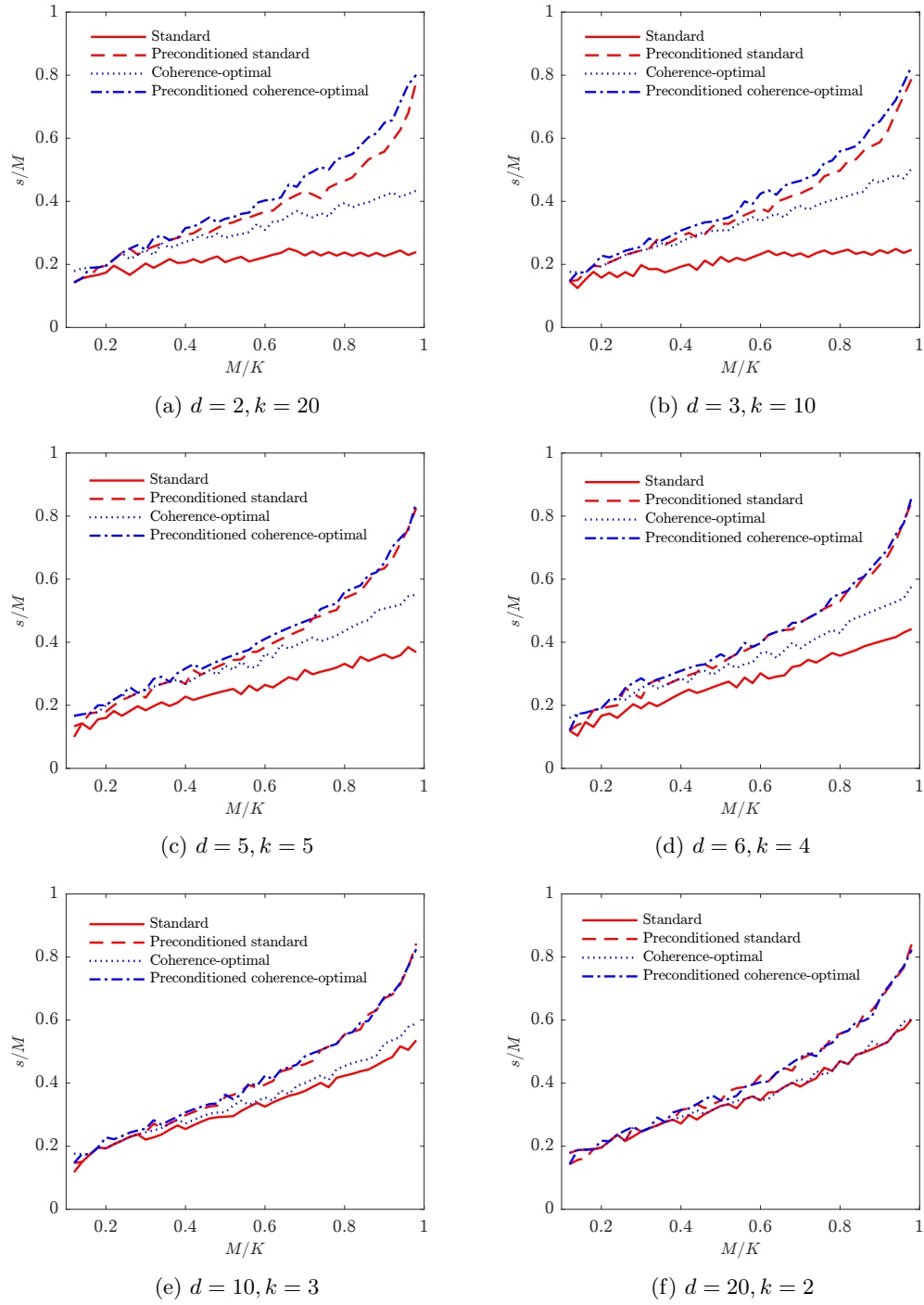


Figure 1: Comparison of phase transition diagrams for standard and coherence-optimal sampling with and without preconditioning for sparse recovery of Legendre-based PCE with various combinations of dimension  $d$  and order  $k$ .

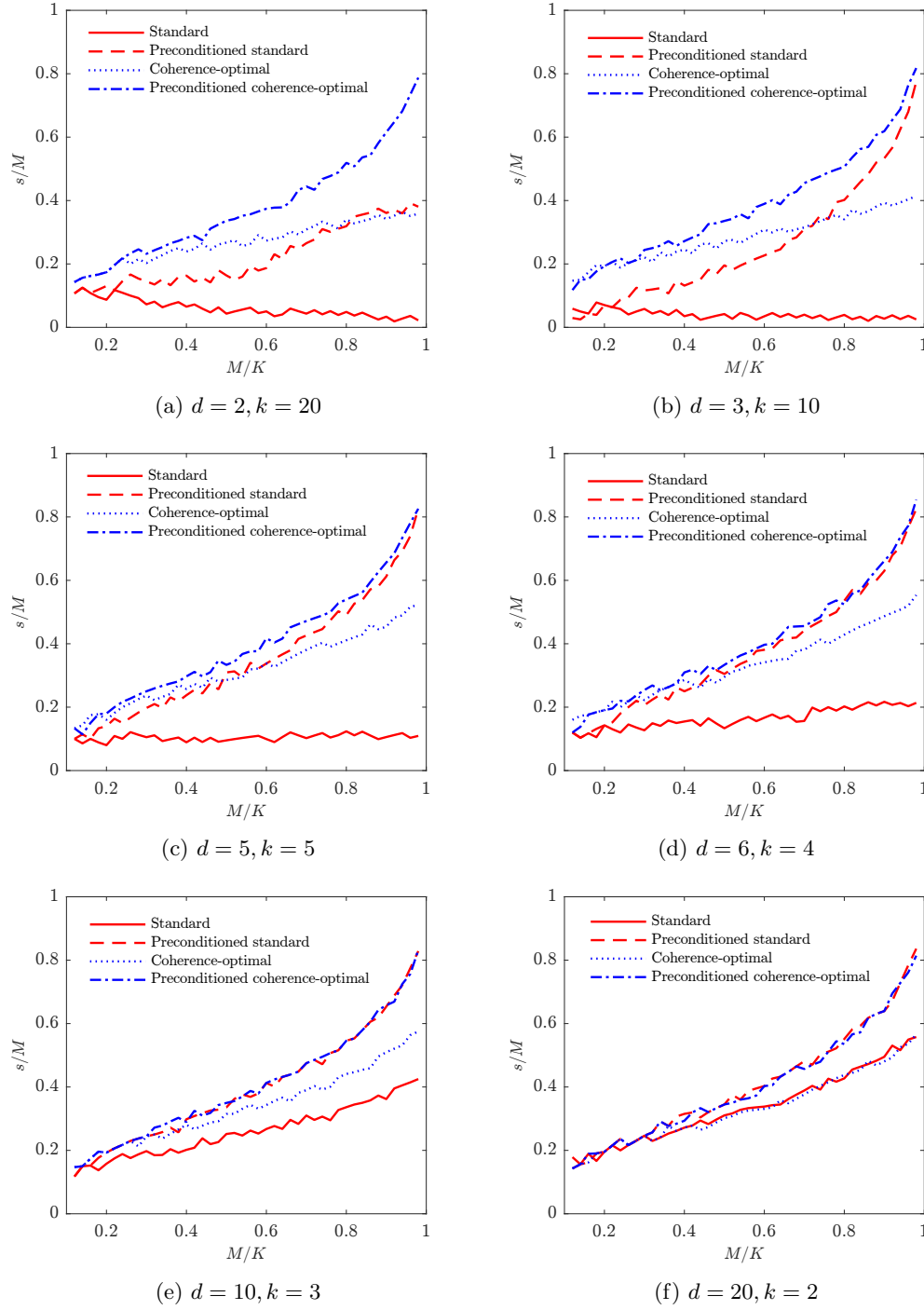


Figure 2: Comparison of phase transition diagrams for standard and coherence-optimal sampling with and without preconditioning for sparse recovery of Hermite-based PCE with various combinations of dimension  $d$  and order  $k$ .

#### 4.2. A low-dimensional high-order polynomial function

Consider the target function,  $u(\Xi)$ , to be a sparse 20th-order Hermite polynomial expansion in a two-dimension random space with standard normal distribution, manufactured according to

$$u(\Xi) = \sum_{i=1}^9 \Xi_1^i \Xi_2^{i+2}. \quad (34)$$

We aim to recover the sparse vector of coefficients using a small set of samples. We compare recovery accuracy for standard sampling and coherence-optimal sampling with and without preconditioning. For all four approaches, we report the performance results obtained by 100 independent runs, each with an independent set of samples. Figure 3a compares the median of relative  $\ell_2$  error, calculated as  $\|\mathbf{c} - \bar{\mathbf{c}}\|_2 / \|\bar{\mathbf{c}}\|_2$ , where  $\bar{\mathbf{c}}$  is the exact coefficient vector and  $\mathbf{c}$  is the solution of the associated  $\ell_1$  minimization. As expected, the preconditioning can be seen to improve the recovery accuracy for both standard and coherence-optimal sampling. Also, as we had concluded from the phase transition diagrams in Figure 2, the preconditioned coherence-optimal sampling results in the most accurate recovery followed by coherence-optimal and preconditioned standard sampling. This is a direct result of improving the orthogonality of measurement matrix using coherence-optimal sampling and preconditioning. To demonstrate these improvements, Figure 3b compares the median of mutual coherence of measurement matrix for all four approaches, and Figure 3c compares the median of average cross-correlation calculated as

$$\gamma(\Psi) := \frac{\|I_K - \tilde{\Psi}^T \tilde{\Psi}\|_F^2}{N}, \quad (35)$$

where  $N := K \times (K - 1)$  is the total number of column pairs. It can be seen that in this example for which  $p \gg d$ , coherence-optimal sampling improves these two orthogonality measures more significantly than preconditioning alone. However, combination of coherence-optimal sampling and preconditioning leads to the most incoherent measurement matrices and most accurate recoveries.

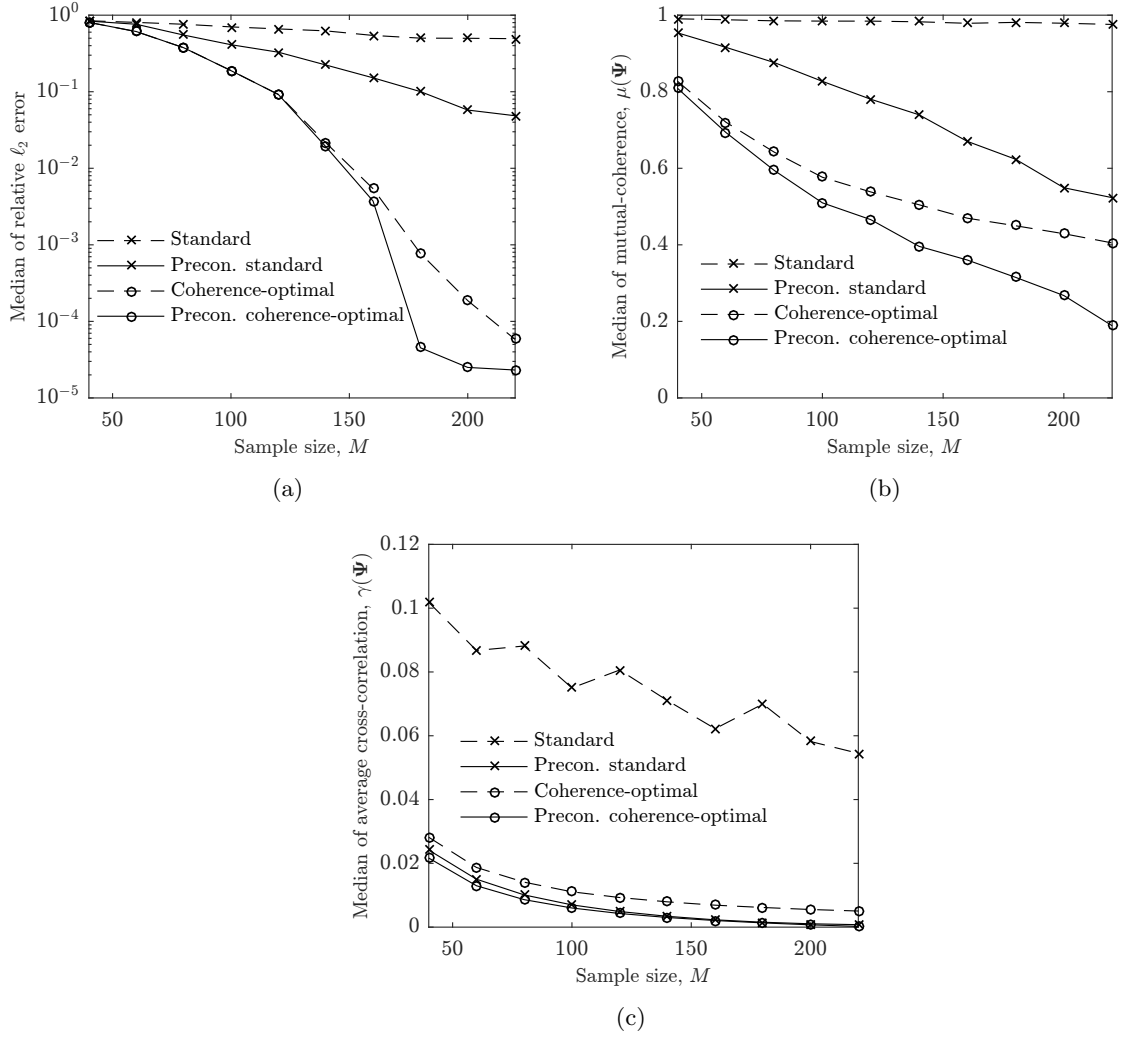


Figure 3: Comparison of results with and without preconditioning for standard and coherence-optimal sampling for low-dimensional high-degree manufactured PCE of Eq. 34. The following measures are compared: (a) median of relative  $\ell_2$  error, (b) success rate, (c) mean of mutual coherence (d) mean of average cross-correlation

#### 4.3. A high-dimensional low-order polynomial function

As a contrasting example, let us consider the target function,  $u(\Xi)$ , to be a sparse second order Legendre polynomial expansion in a 20-dimensional random space with uniform density on  $[-1, 1]^{20}$ , manufactured according to

$$u(\Xi) = \sum_{i=1}^{19} \Xi_i \Xi_{i+1} + \sum_{i=1}^{20} \Xi_i^2. \quad (36)$$

To compare the performance of coherence-optimal and standard sampling with and without preconditioning on this target function, the numerical results were obtained under a setting similar to that in the previous example with 100 independent runs for all the four approaches. Figure 4a compares the medians of relative errors, and Figure 4b compares the success rates for the four approaches. The success rate, here, is defined as the ratio of trials, out of the total of 100, that result in a relative error smaller than  $10^{-7}$ . Figures 4a and 4b show that the improvement in recovery accuracy achieved by coherence-optimal sampling, over standard sampling, is insignificant. However, one can observe that preconditioning successfully improves the recovery accuracy and significantly enhances the success rate. In Figures 4c and 4d, it can be seen that coherence-optimal sampling slightly improves the orthogonality measures, i.e., the mutual coherence and average cross-collaboration, while on the other hand, the preconditioning scheme have significantly improved these measures.

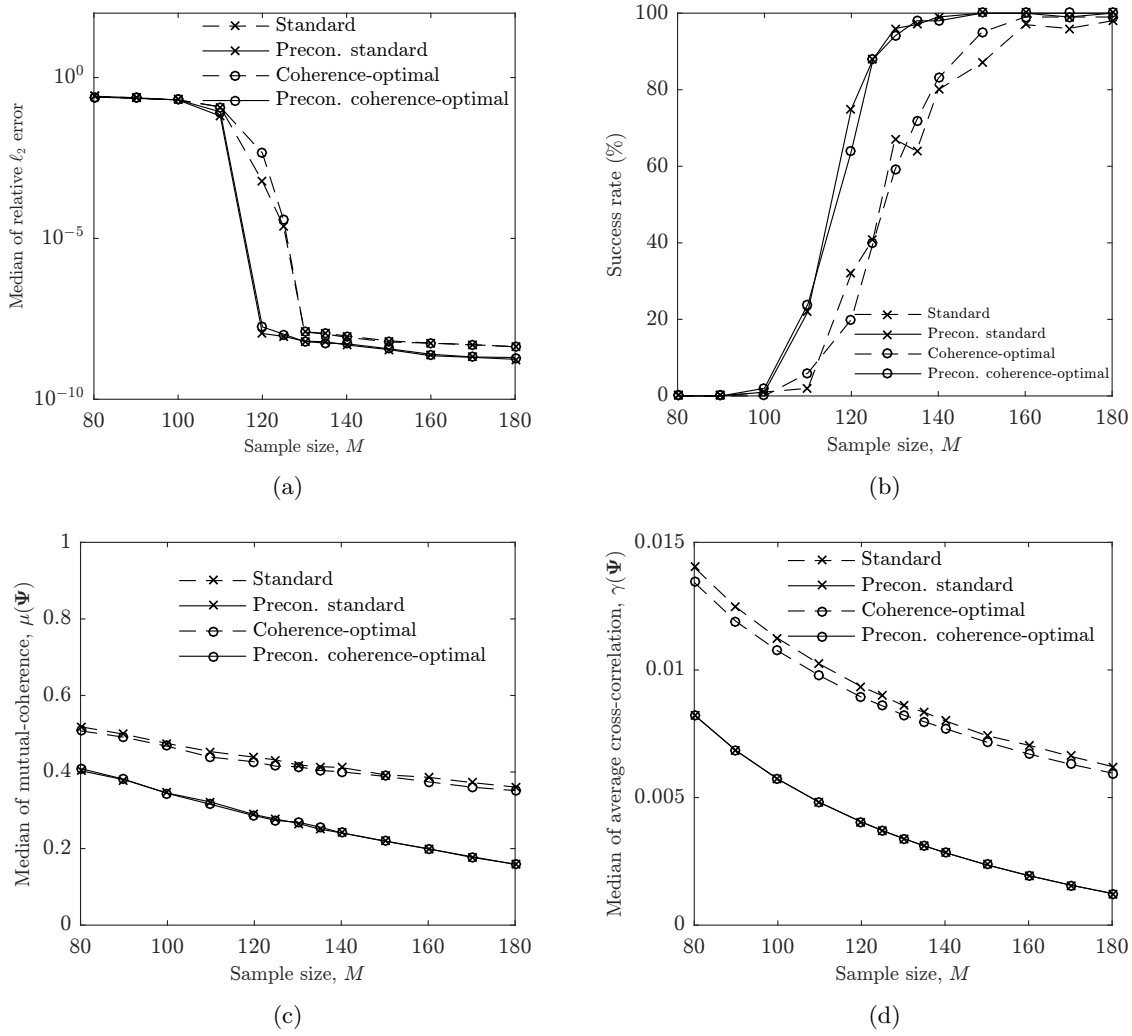


Figure 4: Comparison of results with and without preconditioning for standard and coherence-optimal sampling for the high-dimensional low-degree manufactured PCE of Eq. 36. The following measures are compared: (a) median of relative  $\ell_2$  error, (b) success rate, (c) mean of mutual coherence (d) mean of average cross-correlation

#### 4.4. Six-dimensional generalized Rosenbrock function

The previous two examples were designed to involve “extreme” combinations of dimension and order. As the last example, let us consider a “moderate” combination of dimension and order. Specifically, let us consider the following 6-dimensional generalized Rosenbrock function with random inputs following a uniform density on  $[-1, 1]^6$ ,

$$u(\Xi) = \sum_{i=1}^5 100(\Xi_{i+1} - \Xi_i^2)^2 + (1 - \Xi_i)^2. \quad (37)$$

Similar to the pervious two examples, we report the results for 100 independent trials for standard and coherence-optimal sampling with and without preconditioning. In Figure 5a, it can be seen that preconditioning significantly decreases the median of relative error for standard sampling, also it further improves the recovery accuracy for coherence-optimal sampling. Figure 5a compares the success rates, with the same definition as in Section 4.3, for the four approaches. It can be seen that, preconditioning substantially improves the success rates for both standard and coherence optimal sampling. Finally, Figure 5c and 5d compare the two orthogonality measures, showing that the combined employment of coherence-optimal sampling and preconditioning will result in the best incoherence properties for measurement matrix.

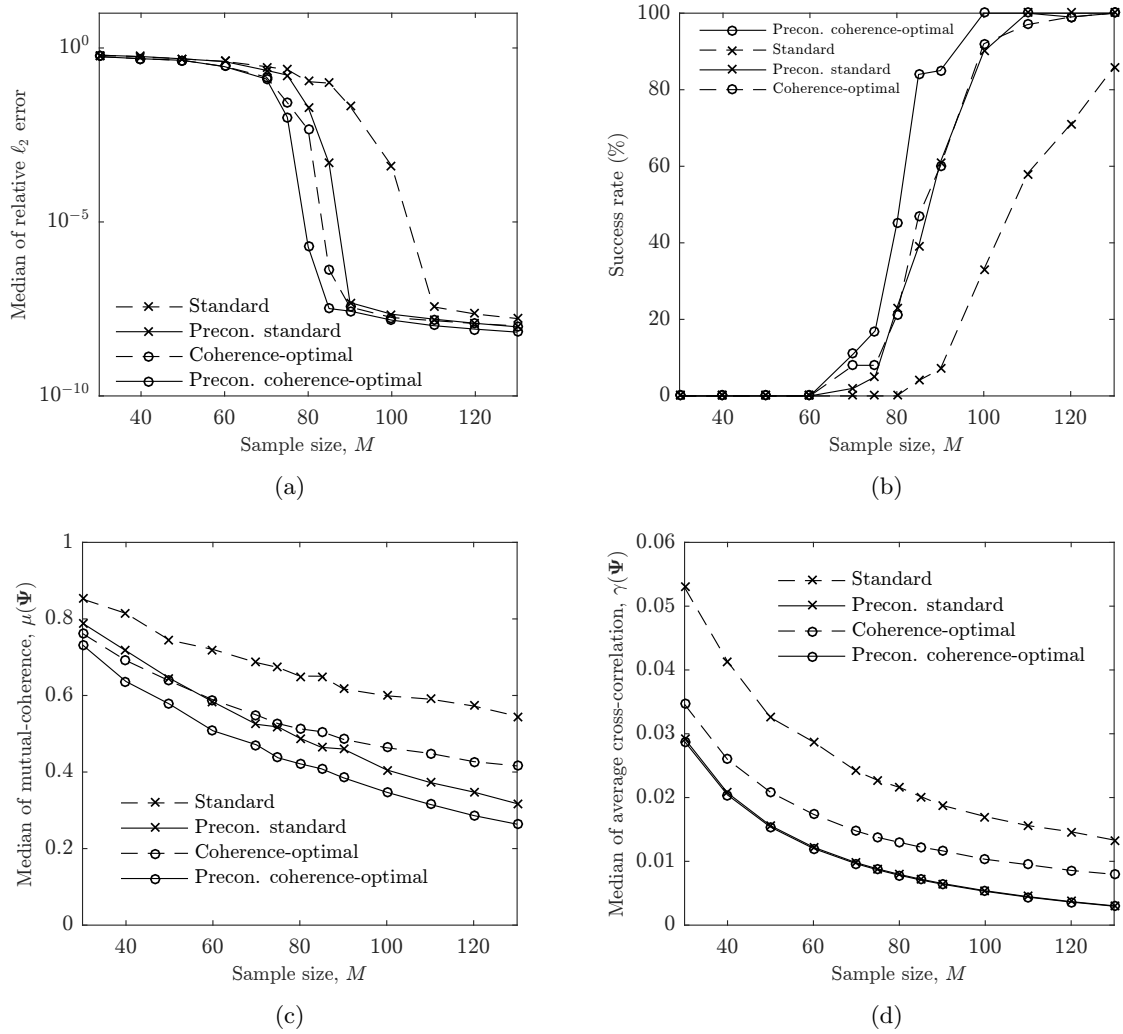


Figure 5: Comparison of results with and without preconditioning for standard and coherence-optimal sampling for Rosenbrock function. The following measures are compared: (a) median of relative  $\ell_2$  error, (b) success rate, (c) mean of mutual coherence (d) mean of average cross-correlation

## 5. Conclusion

In this work, we introduced a preconditioning approach to improve the accuracy of compressive sampling-based recovery of polynomial chaos expansions. Using frameworks proposed for the projection matrix design in signal processing, a design procedure for the preconditioning matrix, to be used in the  $\ell_1$  minimization problem, was studied. We demonstrated the potential accuracy improvement offered solely by preconditioning a measurement matrix that has already been formed, e.g. in cases where samples are already collected. To do this, we multiply both sides of the equation system by a preconditioning matrix such that the preconditioned measurement matrix has better incoherence properties, thereby enhancing the recovery accuracy. We provided theoretical motivation for such scheme along with various numerical examples to validate the preconditioning approach.

It should be noted that there is a vast literature on the design of projection matrix. For instance, recent efforts have been made to optimize projection matrix when the reference signal is not exactly sparse [42, 43] or when the data is noisy [44]. Depending on whether the stochastic problem of interest involves *approximately* sparse expansions or data noise, these two recent works can be used to further improve the introduced preconditioning scheme. Additional studies to evaluate the accuracy gain by such extensions is beyond the scope of this paper and can be addressed in future works.

## 6. References

### References

- [1] P. R. Conrad, Y. M. Marzouk, Adaptive smolyak pseudospectral approximations, *SIAM Journal on Scientific Computing* 35 (6) (2013) A2643–A2670.
- [2] P. G. Constantine, M. S. Eldred, E. T. Phipps, Sparse pseudospectral approximation method, *Computer Methods in Applied Mechanics and Engineering* 229 (2012) 1–12.
- [3] V. Barthelmann, E. Novak, K. Ritter, High dimensional polynomial interpolation on sparse grids, *Advances in Computational Mathematics* 12 (4) (2000) 273–288.
- [4] G. T. Buzzard, Global sensitivity analysis using sparse grid interpolation and polynomial chaos, *Reliability Engineering & System Safety* 107 (2012) 82–89.
- [5] Y. Shin, D. Xiu, Nonadaptive quasi-optimal points selection for least squares linear regression, *SIAM Journal on Scientific Computing* 38 (1) (2016) A385–A411.
- [6] J. Hampton, A. Doostan, Coherence motivated sampling and convergence analysis of least squares polynomial chaos regression, *Computer Methods in Applied Mechanics and Engineering* 290 (2015) 73–97.
- [7] A. Doostan, H. Owhadi, A non-adapted sparse approximation of PDEs with stochastic inputs, *Journal of Computational Physics* 230 (8) (2011) 3015–3034.
- [8] L. Guo, A. Narayan, T. Zhou, Y. Chen, Stochastic collocation methods via  $\ell_1$  minimization using randomized quadratures, *SIAM Journal on Scientific Computing* 39 (1) (2017) A333–A359.
- [9] L. Yan, L. Guo, D. Xiu, Stochastic collocation algorithms using  $\ell_1$  minimization, *International Journal for Uncertainty Quantification* 2 (3).
- [10] N. Alemazkoor, H. Meidani, A near-optimal sampling strategy for sparse recovery of polynomial chaos expansions, *arXiv preprint arXiv:1702.07830*.
- [11] J. Peng, J. Hampton, A. Doostan, A weighted  $\ell_1$ -minimization approach for sparse polynomial chaos expansions, *Journal of Computational Physics* 267 (2014) 92–111.
- [12] L. Yan, Y. Shin, D. Xiu, Sparse approximation using  $\ell_{1-2}$  minimization and its application to stochastic collocation, *SIAM Journal on Scientific Computing* 39 (1) (2017) A229–A254.
- [13] H. Rauhut, R. Ward, Sparse Legendre expansions via  $\ell_1$ -minimization, *Journal of approximation theory* 164 (5) (2012) 517–533.
- [14] G. Tang, G. Iaccarino, Subsampled Gauss quadrature nodes for estimating polynomial chaos expansions, *SIAM/ASA Journal on Uncertainty Quantification* 2 (1) (2014) 423–443.
- [15] J. Hampton, A. Doostan, Compressive sampling of polynomial chaos expansions: convergence analysis and sampling strategies, *Journal of Computational Physics* 280 (2015) 363–386.
- [16] D. Xiu, *Numerical methods for stochastic computations: a spectral method approach*, Princeton University Press, 2010.
- [17] H.-J. Bungartz, M. Griebel, Sparse grids, *Acta numerica* 13 (2004) 147–269.
- [18] Y. Shin, D. Xiu, On a near optimal sampling strategy for least squares polynomial regression, *Journal of Computational Physics* 326 (2016) 931–946.
- [19] J. H. Ender, On compressive sensing applied to radar, *Signal Processing* 90 (5) (2010) 1402–1414.
- [20] J. F. Gemmeke, H. Van Hamme, B. Cranen, L. Boves, Compressive sensing for missing data imputation in noise robust speech recognition, *Selected Topics in Signal Processing, IEEE Journal of* 4 (2) (2010) 272–287.

- [21] M. Lustig, D. Donoho, J. M. Pauly, Sparse MRI: The application of compressed sensing for rapid MR imaging, *Magnetic resonance in medicine* 58 (6) (2007) 1182–1195.
- [22] E. J. Candes, J. K. Romberg, T. Tao, Stable signal recovery from incomplete and inaccurate measurements, *Communications on pure and applied mathematics* 59 (8) (2006) 1207–1223.
- [23] D. L. Donoho, M. Elad, On the stability of the basis pursuit in the presence of noise, *Signal Processing* 86 (3) (2006) 511–532.
- [24] R. Tibshirani, Regression shrinkage and selection via the lasso, *Journal of the Royal Statistical Society. Series B (Methodological)* (1996) 267–288.
- [25] R. Tibshirani, Regression shrinkage and selection via the lasso: a retrospective, *Journal of the Royal Statistical Society: Series B (Statistical Methodology)* 73 (3) (2011) 273–282.
- [26] P. Yin, Y. Lou, Q. He, J. Xin, Minimization of  $\ell_{1-2}$  for compressed sensing, *SIAM Journal on Scientific Computing* 37 (1) (2015) A536–A563.
- [27] Z. Xu, H. Zhang, Y. Wang, X. Chang, Y. Liang,  $\ell_{1/2}$  regularization, *Science China Information Sciences* 53 (6) (2010) 1159–1169.
- [28] E. J. Candès, The restricted isometry property and its implications for compressed sensing, *Comptes Rendus Mathématique* 346 (9) (2008) 589–592.
- [29] H. Rauhut, Compressive sensing and structured random matrices, *Theoretical foundations and numerical methods for sparse recovery* 9 (2010) 1–92.
- [30] J. D. Jakeman, A. Narayan, T. Zhou, A generalized sampling and preconditioning scheme for sparse approximation of polynomial chaos expansions, *SIAM Journal on Scientific Computing* 39 (3) (2017) A1114–A1144.
- [31] D. L. Donoho, M. Elad, V. N. Temlyakov, Stable recovery of sparse overcomplete representations in the presence of noise, *Information Theory, IEEE Transactions on* 52 (1) (2006) 6–18.
- [32] M. Elad, Sparse and redundant representations: From theory to applications in signal and image processing.
- [33] G. Li, Z. Zhu, D. Yang, L. Chang, H. Bai, On projection matrix optimization for compressive sensing systems, *IEEE Transactions on Signal Processing* 61 (11) (2013) 2887–2898.
- [34] M. Elad, Optimized projections for compressed sensing, *IEEE Transactions on Signal Processing* 55 (12) (2007) 5695–5702.
- [35] V. Abolghasemi, S. Ferdowsi, S. Sanei, A gradient-based alternating minimization approach for optimization of the measurement matrix in compressive sensing, *Signal Processing* 92 (4) (2012) 999–1009.
- [36] L. Zelnik-Manor, K. Rosenblum, Y. C. Eldar, Sensing matrix optimization for block-sparse decoding, *IEEE Transactions on Signal Processing* 59 (9) (2011) 4300–4312.
- [37] S. Tian, X. Fan, Z. Li, T. Pan, Y. Choi, H. Sekiya, Orthogonal-gradient measurement matrix construction algorithm, *Chinese Journal of Electronics* 25 (1) (2016) 81–87.
- [38] M. Yaghoobi, L. Daudet, M. E. Davies, Parametric dictionary design for sparse coding, *IEEE Transactions on Signal Processing* 57 (12) (2009) 4800–4810.
- [39] E. Van Den Berg, M. Friedlander, SPGL1: A solver for large-scale sparse reconstruction (2007).
- [40] D. L. Donoho, J. Tanner, Neighborliness of randomly projected simplices in high dimensions, *Proceedings of the National Academy of Sciences of the United States of America* 102 (27) (2005) 9452–9457.
- [41] D. L. Donoho, J. Tanner, Precise undersampling theorems, *Proceedings of the IEEE* 98 (6) (2010) 913–924.



- [42] T. Hong, H. Bai, S. Li, Z. Zhu, An efficient algorithm for designing projection matrix in compressive sensing based on alternating optimization, *Signal Processing* 125 (2016) 9–20.
- [43] T. Hong, Z. Zhu, An efficient method for robust projection matrix design, *arXiv preprint arXiv:1609.08281*.
- [44] A. Shirazinia, S. Dey, Optimized compressed sensing matrix design for noisy communication channels, in: *Communications (ICC), 2015 IEEE International Conference on*, IEEE, 2015, pp. 4547–4552.